Core−Shell Reversion of Hybrid Polymeric Micelles Containing Gold Nanoparticles in the Core

Guoling Hou,[†] Lei Zhu,[‡] Daoyong Chen,*[,†] and Ming Jiang[†]

Department of Macromolecular Science and The Key Laboratory of Molecular Engineering of Polymers, Fudan University, Shanghai 200433, China, and Polymer Program, Department of Chemical, Materials, and Biomolecular Engineering and Institute of Materials Science, University of Connecticut, Storrs, Connecticut 06269

Received October 16, 2006; Revised Manuscript Received December 20, 2006

ABSTRACT: The micellization of polystyrene-*block*-poly(4-vinylpyridine) (PS-*b*-P4VP) in chloroform can be induced by the interaction between P4VP blocks and $HAuCl_4$, forming micelles with PS as the shell and the P4VP/$HAuCl_4$ complex as the core. Subsequent reduction of $HAuCl_4$ leads to hybrid polymeric micelles (HPMs) containing gold nanoparticles (GNs) in the core. In this case, protonation of P4VP block by hydrochloride acid is necessary for the stabilization of HPMs. Further study demonstrates that switching the solvent gradually and continuously from chloroform to a methanol/chloroform (9/1, v/v) mixture, where protonated P4VP is soluble whereas PS is insoluble, leads to a core−shell reversion of the HPMs, forming vesicle-like aggregates with PS as the wall and protonated P4VP/GNs as the shell. The interaction between GNs and protonated pyridine repeating units is a necessary driving force for stable attachment of GNs to shell. When the P4VP block is deprotonated, the GNs will be released from the shell to form precipitates, whereas the vesicles are still stable in the solution. It is also found that during the core−shell reversion the aggregation of PS chains occurs at first among the shell of the HPMs, and then the dissociation of the core happens due to the continuous addition of methanol into the solution, leading to the core−shell reversion. This indicates that there is no intermediate state of the molecularly dispersed block copolymer existing between the HPMs and the RHPMs.

Introduction

Polymeric micelles have attracted considerable attention due to their wide applications such as collection of organic compounds in water,[1] controlled delivery of drugs,[2,3] and nanoreactors for inorganic compounds.[4,5] By using polymeric micelles as nanoreactors to produce metallic nanoparticles **(**MNs**)** within the core, hybrid polymeric micelles (HPMs) can be prepared.[6,7] Usually, to prepare HPMs, polymeric micelles were obtained first, and a precursor of the desired MNs was loaded in the core by means of electrostatic interactions between the core and the precursor. Subsequent reduction of the precursor leads to the formation of HPMs.[6,8] Because the reduction reaction is localized in the nanospace of the core, the size and size distribution of the MNs can be easily controlled.[9,10] In several reported approaches, the loading of the precursor and the formation of polymeric micelles can take place simultaneously.[11−13] In these cases, a block copolymer is dissolved in a common solvent, and the inorganic precursor for the targeted MNs is added, forming complexes with the interacting block. The complexation induces the micellization, forming polymeric micelles with the noninteracting block as the shell and the complexes as the core. Subsequent reduction of the inorganic precursor will lead to the formation of HPMs. In the HPMs formed in a common solvent of the block copolymer precursor, polymeric micelles encapsulating MNs tend to dissociate, when the MNs (whose ability to interact with the interacting block should be quite different from their precursors) interact weakly or do not interact at all with the interacting block. A facile method to stabilize the HPMs is thus desired.

HPMs are promising in applications such as catalysts[14] and biological probes[15] based on the catalytic and photoactivities of the encapsulated MNs.[16] In addition, the polymeric micelles or their analogues with MNs attached to the shell (denoted here as reversed hybrid polymer micelles, RHPMs) are also attractive[17−20] because the soluble hairlike shell makes it easier for the reactants to access to and the products to leave from the MNs such as in a catalytic reaction. Mayer et al. prepared RHPMs by in-situ production of MNs in the presence of amphiphilic block copolymer micelles in water or a polar solvent, and thus formed MNs were anchored to the shell.[18] According to Antonietti et al., these RHPMs are weakly stabilized.[13] Very recently, Ballauff et al. reported the preparation of RHPMs with silver nanoparticles embedded in the thermosensitive PNIPAM shell, and the catalytic activity of the MNs can be controlled by temperature.[21] In all these studies for the preparation RHPMs, the MNs were formed outside the micelle core, and thus the function of using the core as a nanoreactor to control the size and size distribution of MNs is lost.

Ideally, core−shell reversion of the corresponding HPMs can provide a convenient way to prepare RHPMs and allows facile control over the size and size distribution of the MNs by using the core as a nanoreactor. In principle, switching the solvent from a selective solvent for the shell to a selective solvent for the core shall induce core−shell reversion of the HPMs, which will result in RHPMs provided that the interaction between the interacting block and the MNs is strong enough so that they can transform together into the shell of RHPMs. However, this has not been easy practically. Antonietti et al. reported that adding methanol to a *toluene* solution of the HPMs with polystyrene (PS) as the shell and poly(4-vinylpyridine) P4VP/gold nanoparticles (GNs) as the core led to precipitates (this was used to prepare powders of the HPMs),[22] although methanol is a selective solvent for the core. No core−shell reversion was thus obtained in that particular case. We speculate that with the addition of methanol the PS chains aggregated among the

* Corresponding author. E-mail: chendy@fudan.edu.cn.
[†] Fudan University.
[‡] University of Connecticut.

10.1021/ma062373b CCC: $37.00
Published on Web 02/16/2007

Scheme 1. Schematic Description of the Preparation of HPMs, Vesicle-like RHPMs, and Subsequent Release of GNs from the Vesicle-like RHPMs after Deprotonation[a]

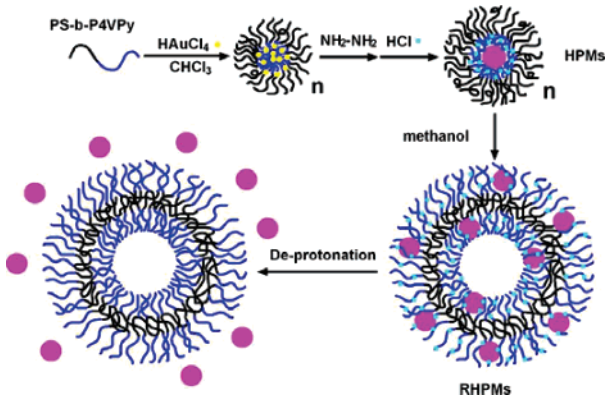

[a] Black solid lines represent PS chains, and blue solid lines represent P4VP chains.

different HPMs and vitrified before dissolution of the P4VP/GNs cores. The vitrified PS aggregates surrounding the core will prohibit the diffusion of the methanol into the core to dissolve P4VP. To achieve core−shell reversion, the dissociation and the dissolution of the core need to occur at least before the vitrification of PS blocks.

In the present study, we report the preparation and the stabilization of HPMs containing gold nanoparticles with a narrow size distribution in the core and the core−shell reversion to form RHPMs, as demonstrated in Scheme 1. The HPMs were prepared by addition of tetrachloroauric acid ($HAuCl_4$) to PS-*b*-P4VP solution in chloroform, a common solvent of both blocks, to form PS shell and P4VP/$HAuCl_4$ core micelles and subsequent reduction of $HAuCl_4$. The HPMs were stabilized by protonation of the core-forming P4VP block chains, since the protonated P4VP were insoluble in chloroform and could bind sufficiently strongly to GNs.[23] The core−shell reversion of the as-prepared HPMs is realized by continuous addition of methanol into the chloroform solution, leading to formation of vesicle-like RHPMs (PS as the wall and protonated P4VP as the shell) with GNs anchored to the shell-forming protonated P4VP chains. We also demonstrate that the protonation of the P4VP chains is necessary for the stabilization of the GNs in the shell of the RHPMs. Once the protonated P4VP block chains are deprotonated, the GNs can be released from the vesicle-like aggregates.

Experimental Section

Materials. The block copolymer PS_{891}-*b*-$P4VP_{311}$ (subscripts indicate the average numbers of the repeat units of the respective blocks; the molecular weight polydispersity $M_w/M_n = 1.13$) was purchased from Polymer Source Inc. Tetrachloroauric acid ($HAuCl_4 \cdot 4H_2O$) (99.9%) was purchased from Shanghai Reagent Co. and hydrazine hydrate ($N_2H_4 \cdot H_2O$, >98%) from Aldrich Chemical Co. Inc. Methanol and chloroform of analytical purity were further purified through desiccation and redistillation. The chloroform used in the present study was added with 1% (v/v) methanol to improve the solubility of the copolymer and $HAuCl_4$.

Micellization of PS-*b*-P4VP/$HAuCl_4$. The block copolymer was dissolved in chloroform [containing 1% (v/v) methanol] for at least 2 days before use. Dynamic light scattering (DLS) measurement indicates that the solution with the copolymer being molecularly dispersed was obtained. Then, $HAuCl_4$ dispersed in the same solvent was added into the copolymer solution under ultrasonication with predetermined molar ratios of $HAuCl_4$/pyridine. The final concentration of the block copolymer is 1 g/L. The mixed solutions were stirred vigorously for several hours before the reduction of $HAuCl_4$.

Preparation of HPMs and Core−Shell Reversion. To each PS-*b*-P4VP/ $HAuCl_4$ solution, 10-fold hydrazine hydrate was added. Immediately, a purple red color appeared. After 30 min, concentrated hydrochloride acid (38%) with a molar ratio of HCl to hydrazine hydrate of 4:1 was added. The solution of the HPMs with PS being the shell and the protonated P4VP/GNs being the core were thus prepared. In this study, only the solution with a molar ratio of $HAuCl_4$/pyridine of 0.3 was used for the core−shell reversion. Before the core−shell reversion, the solution was diluted to a concentration of the block copolymer of 0.1 g/L. The concentration of $HAuCl_4$ in the diluted solution is thus 0.25 g/L, and the solid content is 0.35 g/L. To induce core−shell reversion, methanol was added dropwise to the solution until a volume ratio of methanol/chloroform reached 9/1.

Preparation of PS-*b*-P4VP/HCl Micelles and the Core−Shell Reversion. After the complete dissolution of PS_{891}-*b*-$P4VP_{311}$ in chloroform [containing 1% (v/v) methanol], the micellization of the block copolymer was induced by addition of excess (the molar ratio of HCl to the pyridine units is 10:1) hydrochloric acid (38%) under ultrasonic vibration. The core−shell reversion of PS-*b*-P4VP/HCl micelles was conducted by adding methanol to the solution in chloroform until a volume ratio of methanol/chloroform reached 9/1.

Laser Light Scattering (LLS). A modified commercial light scattering spectrometer (ALV/SP-125) equipped with an ALV-5000 multi-τ digital time correlator and an ADLAS DPY425 II solid-state laser (output power = 400 mW at $\lambda = 532$ nm) was used. In dynamic LLS (DLS), the line-width distribution $G(\Gamma)$ can be calculated from the Laplace reversion of intensity−intensity time correlation function $G^{(2)}(q,t)$. The reversion was carried out by the CONTIN program. $G(\Gamma)$ can be converted into a transitional diffusion coefficient distribution $G(D)$ or a hydrodynamic radius distribution $f(R_h)$ via the Stokes−Einstein equation, $R_h = (k_BT/6\pi\eta)D^{-1}$, where k_B, T, and η are the Boltzmann constant, the absolute temperature in kelvin, and the solvent viscosity, respectively. All the DLS measurements were performed at 25 ± 0.1 °C and at a scattering angle between 15° and 150° for the HPMs or between 15° and 90° for the RHPMs. No remarkable scattering angle dependence of the $\langle R_h \rangle$ was observed. All the micelle solutions were measured directly without further dilution, and the solutions were cleaned using a 0.45 μm Millipore filter before measurements. In static light scattering (SLS), angular dependence of the excess absolute time-averaged scattered intensity of a dilute dispersion, i.e., the Rayleigh ratio $R_{vv}(q)$, can lead to the z-averaged root-mean-square radius of gyration $\langle R_g^2 \rangle_z^{1/2}$, where q is the scattering vector.

UV−Vis Spectroscopy. UV−vis spectroscopy was carried out on a Perkin-Elmer Lambda 35 UV−vis absorption spectrometer. Quartz cells were used for the measurements.

Transmission Electron Microscopy (TEM). TEM observations were conducted on a Philips CM120 electron microscope at an acceleration voltage of 80 kV. The samples for the TEM observations were prepared by placing a drop of the micelle solution on carbon-coated copper grids. After solvent evaporation, the sample was observed in TEM without further treatment.

^{1}H NMR Measurements. ^{1}H NMR measurements were performed on a Bruker DMX500 spectrometer with tetramethylsilane (TMS) as an internal reference.

X-ray Diffraction (XRD) Analysis. Reflection-mode X-ray diffraction (XRD) was recorded on an X'PertPro diffractometer (PANalytic) with an X-ray tube generator, operating at 40 kV and 40 mA. Cu Kα radiation ($\lambda = 0.1542$ nm) and a graphite monochromator were used in the experiment. The detector used is X'Celerator. The scattering angle 2θ scanning rate was 0.02°/s in a range of 20−90°. Thin film sample was prepared by casting the HPM solution onto a piece of silica wafer.

Results and Discussion

I. Formation of Au-Containing PS-*b*-P4VP Micelles. As reported in our previous studies,[24,25] PS-*b*-P4VP can be molecularly dispersed in chloroform/methanol (99/1, v/v). Since

Table 1. Dynamic Light Scattering Characterization Data of PS-*b*-P4VP/$HAuCl_4$ Aggregates Formed in Chloroform

MR	$\langle D_h \rangle$/nm[a]	$\mu_2/\langle\Gamma\rangle^2$ [b]
0.1	64	0.129
0.3	68	0.132
0.5	82	0.207
>0.5	ND[c]	ND

[a] Average hydrodynamic diameter of the aggregates. [b] Polydispersity index of the size distribution.[26] [c] Not determined.

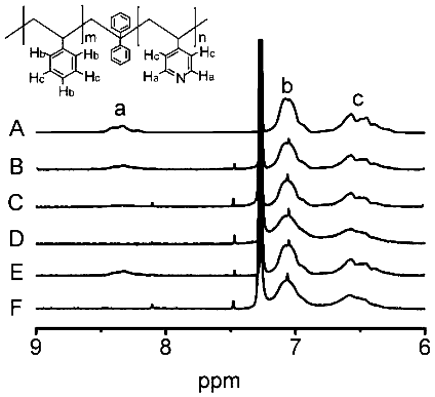

Figure 1. ^1H NMR spectra of the neat block copolymer (A), PS-*b*-P4VP/$HAuCl_4$ complexes at MR of 0.1 (B), 0.3 (C), and 0.5 (D), and PS-*b*-P4VP/GNs obtained by reduction of PS-*b*-P4VP/$HAuCl_4$ at MR of 0.3 without further protonation (E) and with protonation (F) in deuterated chloroform containing 1% (v/v) deuterated methanol using TMS as an internal standard. The inset shows the chemical structure of the block copolymer with ^1H assignments, a−c, in the spectra.

the presence of 1% methanol has no significant effect on the physical properties of the solution, for simplicity of description, the mixed solvent is denoted as chloroform in the text below. It was reported that addition of formic acid or perfluorooctanoic acid to PS-*b*-P4VP solution in chloroform led to polymeric micelles with PS being the shell and P4VP/formic acid or P4VP/perfluorooctanoic acid complexes being the core.[24,25] In the present study, mixing PS_{891}-*b*-$P4VP_{311}$ and $HAuCl_4$ in chloroform also resulted in micellization of the block copolymer. The aggregates formed at different molar ratios (MRs) of $HAuCl_4$ to pyridine were characterized by dynamic light scattering (DLS).

As shown in Table 1, when MR ≤ 0.5, the average hydrodynamic diameters $\langle D_h \rangle$ of the aggregates are between 64 and 82 nm. These aggregates are quite stable because no obvious changes are detected by DLS during the storage for weeks. However, the aggregates formed at MR > 0.5 are unstable and precipitate from the solution several hours after preparation. The as-prepared PS-*b*-P4VP/$HAuCl_4$ aggregates are further characterized by ^1H NMR.

The ^1H NMR spectra of PS-*b*-P4VP/$HAuCl_4$ complexes at the MRs of 0.0, 0.1, 0.3, and 0.5 in deuterated chloroform containing 1.0% (v/v) deuterated methanol are shown in Figure 1A−D. For clarity, only the spectra from 6.0 to 9.0 ppm are presented with peak assignments denoted as a, b, and c. Peak b is assigned to the hydrogen atoms H_b in the benzene rings, and peaks a and c are associated with H_a in pyridine rings and H_c in both the pyridine and benzene rings, respectively.[27] In the spectrum of the neat block copolymer (spectrum A in Figure 1), the signals from both the benzene and pyridine rings can be clearly seen. However, in the spectra of PS-*b*-P4VP/$HAuCl_4$ at MR of 0.3 and 0.5 (spectra C and D), peak a associated with the pyridine rings disappears, and the signal assigned to H_c in the pyridine rings must also disappear because the intensity ratio of peak c to peak b decreases to ca. 2/3, corresponding to the

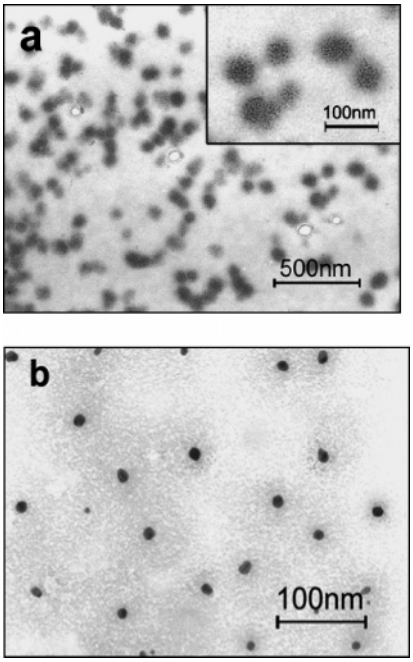

Figure 2. TEM images of (a) PS-*b*-P4VP/$HAuCl_4$ micelles and (b) HPMs at a MR of 0.3. The inset in (a) shows aggregates at a higher magnification. The HPMs for TEM observations were stabilized by adding hydrochloride acid into the solution 30 min after the addition of NH_2NH_2.

molar ratio of H_c to H_b in the benzene rings. On the contrary, the relative intensity of peak b, which is assigned to the H_b in the benzene rings only, does not change. The disappearance of pyridine signals indicates a complete loss of mobility of the P4VP blocks, suggesting P4VP aggregation into a core. On the other hand, the invariant relative intensities of the H_b and H_c signals in the benzene rings reflect good solubility of the PS blocks. These results confirm the core−shell structure of PS-*b*-P4VP/$HAuCl_4$ aggregates with PS blocks being the shell and P4VP/$HAuCl_4$ complexes being the core.[24,25] On the basis of previous studies, complexation can occur between pyridine in the P4VP blocks and $HAuCl_4$.[24,25] The resultant pyridine/$HAuCl_4$ complex has a high polarity and thus becomes insoluble in low-polarity solvents such as chloroform, leading to micellization of the block copolymer. Therefore, the complexation between $HAuCl_4$ and P4VP blocks is the driving force for micellization of PS-*b*-P4VP in chloroform. The block copolymer micellization in such a mechanism also encapsulates the complexed $HAuCl_4$ molecules within the core. When MR is 0.1, peak a is still visible in spectrum B of Figure 1, although its relative intensity decreases as compared with that of the pure PS-*b*-P4VP (spectrum A in Figure 1). This can be attributed to either uncomplexed soluble pyridine units in the core (i.e., the core is swollen by the solvent; the micelles with a swollen core were confirmed previously[28]) or some molecularly solubilized copolymer chains in the solution, or both.

A TEM image of PS-*b*-P4VP/$HAuCl_4$ aggregates at a MR of 0.3 is shown in Figure 2a. They are spherical aggregates. The core−shell structure is visible in the TEM image with a higher magnification (the inset in Figure 2a). From the inset in Figure 2a, we can see that the cores appear darker, indicating the encapsulation of $HAuCl_4$ in the core. The cores are surrounded by a faint gray peripheral layer, which can be attributed to a PS shell. The average diameter of the particles is about 60 nm, close to the size measured by DLS. Experimental results also show that when MR is 0.5, the PS-*b*-P4VP/$HAuCl_4$ aggregates are irregular; when MR is 0.1, the irregular

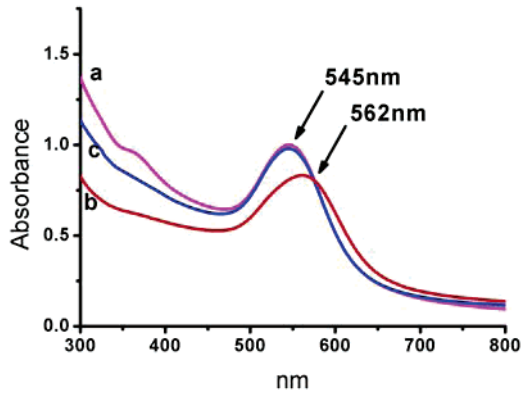

Figure 3. UV−vis spectra for the HPMs at MR = 0.3 measured (a) 30 min and (b) 24 h after addition of hydrazine hydrate. (c) Measurement is taken 24 h after addition of hydrochloric acid, which is added 30 min after the addition of hydrazine hydrate.

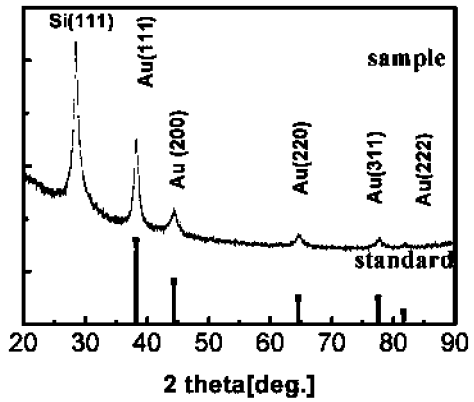

Figure 4. X-ray diffraction profile of the GNs in PS-*b*-P4VP micelles. The vertical lines at the bottom are the reference data for the bulk Au crystals taken from the powder diffraction file JCPDS Card, No. 89-3697.

aggregates of a low contrast, attributed to molecularly dispersed uncomplexed copolymer chains that aggregate together after the drying, coexist with the PS-*b*-P4VP/$HAuCl_4$ aggregates (data not shown). The solution of PS-*b*-P4VP/$HAuCl_4$ aggregates at the MR of 0.3 was selected for further study.

For a complete and rapid reduction of the $HAuCl_4$ encapsulated in the core, 10-fold of hydrazine hydrate was added into the chloroform solution containing PS-*b*-P4VP/$HAuCl_4$ at a MR of 0.3. On the basis of previous studies, a reaction time of 30 min is *enough* for the reduction reaction.[29] The HPMs are thus produced. The UV−vis spectrum of the HPMs measured 30 min after the addition of NH_2-NH_2 is shown as curve a in Figure 3. However, we found that the UV−vis spectrum of the solution after the complete reduction still changed with time. As shown in spectrum b, the absorption peak red-shifts considerably 24 h after the addition of NH_2-NH_2, as compared with spectrum a. The red shift in absorption should result from the aggregation among the GNs. It is noted that excess hydrazine hydrate leads to deprotonation of the pyridine units in P4VP chains, which eventually become soluble in the solution. After deprotonation, the micelles tend to dissociate. This is verified by the fact that the signals of P4VP chains appear again in the ^1H NMR spectrum of the HPMs after the addition of excess hydrazine hydrate (spectrum E, Figure 1). Naturally, without further protection by the surrounding polymeric micelles, the GNs will aggregate together and are observed to precipitate out of the solution in less than 3 days after the preparation. We found that the dissociation of the micelles and the aggregation between the GNs could be effectively prohibited by a timely addition of hydrochloric acid into the solution (HCl/NH_2NH_2 = 4:1). Spectrum c in Figure 3 shows the same absorption peak as that in spectrum a, indicating that the addition of hydrochloric acid into the solution 30 min after the introduction of NH_2-NH_2 stabilizes the micellar aggregates, and no GN aggregation was detected. ^1H NMR characterization (spectrum F, Figure 1) confirms that after the addition of excess hydrochloric acid all the pyridine signals are undetectable because the P4VP chains are protonated and then aggregated together. Furthermore, TEM observations show no aggregation among the GNs (Figure 2b). It was mentioned by Mossmer et al.[29] that in the system of PS-*b*-P2VP/GNs in toluene the protonation is necessary for the stabilization of GNs within the core, although the core formed by P2VP in toluene without protonation is already in an aggregated state. We believe that there is a binding interaction between protonated pyridine groups and naked GNs, which is helpful to stabilize GNs in the cores of the HPMs. This is consistent with the fact that cetyltrimethylammonium bromide (CTAB) can be used as a phase-transfer agent to transfer GNs from an aqueous phase into a hydrophobic phase.[23]

The stabilized HPMs were measured by DLS. In principle, considering a PS-*b*-P4VP/$HAuCl_4$ micelle, the reduction will lead to the transformation of $HAuCl_4$ molecules into Au atoms that coagulate to form an Au nanoparticle in the core. This should result in a slight shrink of the micelle. However, in the present study, the $\langle D_h \rangle$ of the resultant HPMs increases to 116 nm (the $\langle D_h \rangle$ of the PS-*b*-P4VP/$HAuCl_4$ micelles is 68 nm; Table 1). Our explanation is: for the reduction of $HAuCl_4$ and the stabilization of the HPMs, in the present study, the amounts of hydrazine hydrate, the aqueous solution of HCl (containing 72% water) added to a chloroform solution containing 2.6 mg of the PS-*b*-P4VP/$HAuCl_4$ micelles, are 0.56 and 1.6 mg, respectively. These materials should mostly exist in the core of the HPMs that is with a high polarity formed by the protonated P4VP block chains. The entrance of water molecules into the polar core of polymeric micelles dispersed in a low-polarity solvent was reported by Eisenberg et al.[30] The existence of these materials in the core certainly increases the $\langle D_h \rangle$ of the resultant HPMs remarkably. We failed to measure them by the liquid ^1H NMR measurements since the core is rigid.[27]

The stabilized HPMs were observed using TEM as well. The reduction of PS-*b*-P4VP/$HAuCl_4$ at a MR of 0.3 by hydrazine hydrate leads to the GNs with an average diameter of 15 nm (Figure 2b). From Figure 2b, the GNs are localized in the center of the polymeric micelles, and without staining the polymeric micelles show a low contrast in the TEM image. In Figure 4 the XRD profile of the HPMs exhibits five Bragg diffraction peaks at 38.36°, 44.45°, 64.62°, 77.84°, and 81.86°, corresponding to the (111), (200), (220), (311), and (222) diffractions of a conventional cubic phase of Au, respectively.[31] As expected, the XRD peaks of nanocrystallites were considerably broadened, compared to those of the bulk Au, because of the small size of the Au crystallites. The average sizes of the Au particles produced in the core of PS-*b*-P4VP/$HAuCl_4$ micelles are estimated to be 13.5 nm according to the Debye−Scherrer equation,[31] which are close to the value observed by TEM. These results suggest that each of the HPMs contains a single gold nanoparticle in the core. In other words, cherry-like HPMs are produced.[22,32]

II. Core−Shell Reversion of HPMs To Form RHPMs with a Vesicle-like Morphology. As mentioned before, the RHPMs having GNs in the shell may have unique properties, especially when they are used as homogeneous catalysts.[14,19,20] In addition, if we prepare RHPMs via core−shell reversion of HPMs, the

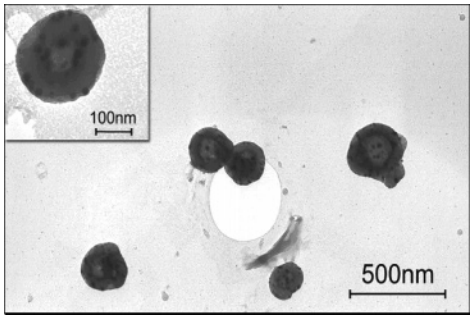

Figure 5. TEM images of reversed PS-*b*-P4VP micelles containing gold nanoparticles in the shell.

size and size distribution of the targeted MNs can be well-controlled because they are produced in the core of the HPMs. In our further effort to realize the core−shell reversion of the HPMs, methanol, a selective solvent for the core, was used. When the addition of methanol into the HPMs (with protonated P4VP blocks) in chloroform reached a volume ratio (VR) of methanol/chloroform between 1:3 and 1:1, the solution becomes slightly turbid. However, continuous addition of methanol leads to the disappearance of the turbidity. The solution at a VR of 9:1 is very stable, and no precipitation was observed during storage for months. This solution was characterized by UV−vis spectroscopy. The absorption peak of GNs is at 538 nm, indicating a remarkable change in the medium surrounding the GNs, and does not change during the storage for weeks. Our control experiments indicate that PS-*b*-P4VP will self-assemble in the mixed solvent, forming micelles with PS being the core and P4VP being the shell, no matter whether P4VP block is protonated or not, indicating that the mixed solvent is a selective solvent for either P4VP or protonated P4VP blocks. As a result, RHPMs are produced with the protonated P4VP/GNs being the shell and PS being the core or wall of vesicle-like aggregates. This conclusion is supported by the results of the TEM observations and the ^{1}H NMR characterization below.

The aggregates formed at a VR of 9:1 were observed by TEM. A typical TEM image is shown in Figure 5. Vesicle-like morphology is seen. The location of the GNs observed by TEM suggests that the GNs are mostly anchored to the shell of the vesicle-like aggregates. In the TEM image of the RHPMs, the average size of GNs seems larger than that observed in the TEM image of the HPMs and that determined by XRD. It is possible that some of GNs may aggregate together to form larger Au nanoparticles during the core−shell reversion. In the cherry-like HPMs containing one Au nanoparticle each, the Au nanoparticles were isolated and cannot aggregate with each other. However, during the core−shell reversion, the Au nanoparticles have chances to meet and aggregate with each other. The vesicle-like morphology of the aggregates is further supported by light scattering measurements. The $\langle R_g \rangle$ (the average diameter of gyration) and $\langle R_h \rangle$ (measured at a scattering angle of 15°) are 329 and 280 nm, respectively, and the $\langle R_g \rangle / \langle R_h \rangle$ is 1.17. Theoretically, for a uniform nondraining solid sphere, a nondraining thin shell vesicle, and a random coil, the ratios of $\langle R_g \rangle / \langle R_h \rangle$ are 0.774, 1.0, and 1.5−1.8, respectively.[33] Experimentally, $\langle R_g \rangle / \langle R_h \rangle$ is often less than 0.774 for a polymeric micelle, since the density of the core is remarkably higher than that of the shell. For a polymeric vesicle or a hollow sphere, $\langle R_g \rangle / \langle R_h \rangle$ may be less or greater than 1.0, depending on the thickness and the density of the wall.[25] The fact that $\langle R_g \rangle / \langle R_h \rangle$ is 1.17 is consistent with the vesicle-like morphology of the aggregates observed by TEM.[25] Note that the average size of the RHPMs observed by TEM (ca. 250 nm) is much less than

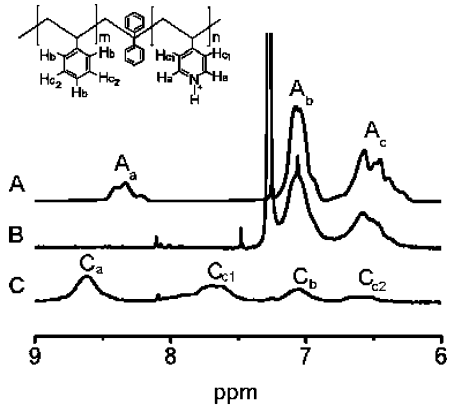

Figure 6. ^{1}H NMR spectra of PS_{891}-*b*-$P4VP_{311}$ block copolymer (A), the hybrid polymeric micelles (HPMs) with PS as the shell and protonated P4VP encapsulating GNs as the core (B), and the aggregates after the core−shell reversion (C). The assignments for spectra A and B are given as the inset in Figure 1. The inset in this figure is the assignments for spectrum C. In spectrum C, the signals C_a, C_{c1}, C_b, and C_{c2} are attributed to H_a, H_{c1}, H_b, and H_{c2} in the inset structure, respectively.

that measured by DLS. This implies that the aggregates are somewhat swollen in the mixed solution because of the existence of 10% (v/v) chloroform, while the dried aggregates have a remarkably contracted size.

As mentioned before, ^{1}H NMR characterization can give us information concerning the core−shell structure of the block copolymer micelles. For the ^{1}H NMR characterization, the original solution of the RHPMs was dried and subsequently dissolved by deuterated methanol/deuterated chloroform mixture (9/1, v/v) to a block copolymer concentration of 1 g/L. The ^{1}H NMR spectrum for the RHPMs is presented in Figure 6 as spectrum C. For comparison, the spectra of the pure PS-*b*-P4VP (spectrum A) and the HPMs in deuterated chloroform (spectrum B) are also presented in Figure 6. Spectrum C exhibits signals of protonated pyridine rings (peaks C_a and C_{c1}) and the benzene rings (peaks C_b and C_{c2}). Compared with spectrum B, signals from protonated P4VP chains are still visible (the assignments for spectrum C are presented as an inset in Figure 6), indicating that the protonated P4VP chains are solubilized by the mixed solvent. Although the signals attributed to PS chains (peaks C_b and C_{c2}, assigned to the H_b and H_{c2} in the benzene rings, respectively) are still visible, the intensity ratio of peak C_{c2} to peak C_{c1} is only 0.22:1, much less than the actual molar ratio of H_{c1} to H_{c2} (see the inset in Figure 6) in the PS_{891}-*b*-$P4VP_{311}$, which should be (891*2)/(311*2) = 2.86. Assuming that all the pyridine rings are protonated and contribute to the signals in the spectrum C, only 7.6% of benzene rings are detectable in the ^{1}H NMR measurement. This indicates that most of benzene rings of PS chains are aggregated. We speculate that the existence of 10% (v/v) chloroform in the solution should be responsible for the signals from the wall-forming PS chains. We can thus conclude that the vesicle-like aggregates in methanol/chloroform have protonated P4VP chains as the shell and PS as the wall. The anchoring of GNs to the protonated P4VP chains as the shell of the RHPMs is reasonable since they can interact with the protonated pyridine rings but cannot interact with PS chains. We also demonstrate that when the solution of the RHPMs is added with hydrazine hydrate to deprotonate the P4VP chains, the solution becomes colorless in a short time, indicating that all the GNs have been released from the shell and precipitate out of solution. This is because the driving force for the attachment of Au nanoparticles in the shell of the RHPMs is the binding interaction between the

protonated pyridine units and Au nanoparticles.[23] On the basis of present study and the results obtained by Mossmer et al.,[29] the interaction between (unprotonated) pyridine groups and Au nanoparticles is not strong enough to keep the attachment of Au nanoparticles with unprotonated P4VP chains. After addition of hydrazine hydrate into the solution of the RHPMs, the protonated pyridine groups in the shell are changed to unprotonated ones, and the Au nanoparticles are released from the shell of the RHPMs formed by unprotonated P4VP blocks. Once the Au nanoparticles are released, they will aggregate with each other and precipitate out of the solution. After the release of the gold nanoparticles, the vesicle-like aggregates are still stabilized in the solution. We measured the size of the RHPMs after the deprotonation and the release of the GNs by DLS and found that the $\langle D_h \rangle$ increases to 351 nm. Our TEM observation found some irregular aggregates with a size larger than that of the RHPMs. It seems that the deprotonation and the release of GNs have complicated effects on the size and the shape of the RHPMs. It is confirmed that protonation of the P4VP blocks is necessary for the stable attachment of GNs in the shell of the vesicle-like aggregates.

Polymer concentration has a pronounced effect on successful core−shell reversion. In fact, the core−shell reversion can be realized only when the concentration of the PS_{891}-*b*-$P4VP_{311}$ is lower than or equal to 0.1 g/L. Otherwise, the addition of the methanol into the solution of the HPMs will result in precipitation.

It is noted in the present study that when the methanol is added to the HPMs in chloroform at a low VR of methanol to chloroform between 1:3 and 1:1, the solution becomes turbid, indicating the PS chains begin to aggregate. Standing these solutions for several hours leads to precipitation. Once the precipitate is formed, it cannot be redissolved by further addition of methanol. This is because the aggregated PS chains are vitrified during the standing, and the vitrified PS chains surrounding the core prohibit the diffusion of methanol into the core to dissolve the protonated P4VP. Nevertheless, the PS vitrification takes place in at least several hours after the aggregation. Continuous addition of methanol (i.e., without standing over hours) from the VR = 0 to 9:1 will lead to the core−shell reversion. We speculate that before vitrification PS chains should be loosely associated in the normal HPMs, and thus diffusion of methanol into the cores to solubilize protonated P4VP is still possible. Therefore, continuous addition of methanol into the solutions can cause the core−shell reversion to form RHPMs. As the PS chains aggregate before the dissolution of the core-forming protonated P4VP chains, there should be no intermediate state that the block copolymer is molecularly dispersed in the solution between the HPMs and the RHPMs during the core−shell reversion (this phenomenon has not been reported before, to our knowledge) although the state of the aggregates at a VR between 1:3 and 1:1 can be thought as one of the intermediate states during the core−shell revision.

We think that whether the core−shell reversion can be realized by adding methanol into the solution of PS shell and protonated P4VP/GN core micelles (HPMs) in chloroform is determined by the competition between the aggregation and vitrification of the PS chains and the dissolution of the core. Generally speaking, the speed of the aggregation and vitrification of PS chains depends on the molecular weight of the PS chains and the concentration of the block copolymer (the precursor of the HPMs and the RHPMs). Decreasing the molecular weight of PS block and/or the concentration of the block copolymer

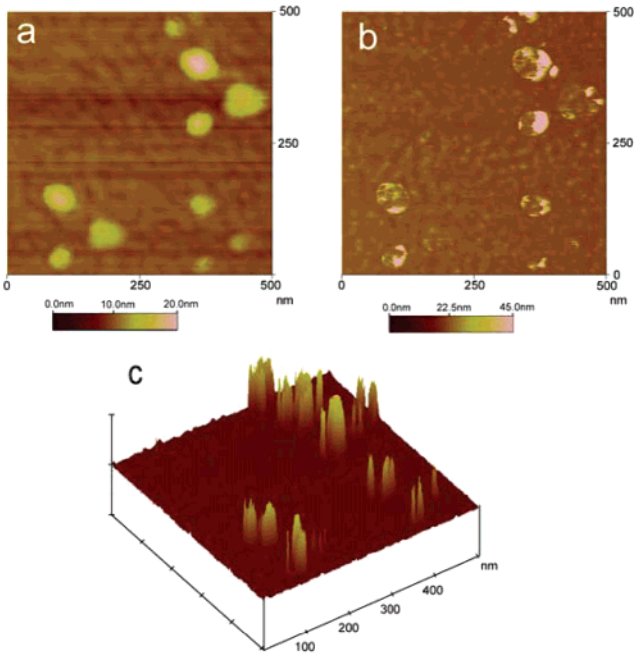

Figure 7. AFM height images of the HPMs prepared from PS87-*b*-P4VP112 at a MR of 0.3 (a), the 2D phase image (b), and the 3D phase image (c) of the RHPMs prepared via core−shell reversion of the HPMs.

can decrease the speed of aggregation and vitrification of PS chains. When PS-*b*-P4VP with a higher molecular weight PS block is used, as in the case of PS_{891}-*b*-$P4VP_{311}$, the core−shell reversion can only be conducted at a lower concentration of the block copolymer. When PS-*b*-P4VP with a lower molecular weight PS block is used, the core−shell reversion should be able to be carried out at a higher concentration of the block copolymer. On the basis of this consideration, we also used PS_{87}-*b*-$P4VP_{112}$ (Polymer Source Inc., $M_w/M_n = 1.09$) for the core−shell reversion study. The HPMs at a MR of $HAuCl_4$ to pyridine of 0.3 (Figure 7a) were prepared on the basis of the same procedures. The core−shell reversion can be achieved at a block copolymer concentration of 1 g/L via an almost identical procedures. We also observe that when methanol is added to the HPMs in chloroform at a low VR of methanol to chloroform (about 1:1), the solution becomes turbid. Standing this solution for several hours leads to the formation of precipitates. Once the precipitates are formed, they cannot be redissolved by further addition of methanol. The turbidity should result from a loose aggregation of PS chains because continuous addition (i.e., without the standing for hours) of methanol into the solution can lead to the core−shell reversion. Different from the case of PS_{891}-*b*-$P4VP_{311}$, the core−shell reversed aggregates (Figure 7b) have a size close to that of the HPMs (Figure 7a). The locations of GNs in the RHPMs derived from PS_{87}-*b*-$P4VP_{112}$ are identified by the remarkable difference in the modulus between GNs and their surrounding polymeric components, as is indicated in the 3D AFM phase image of the RHPMs (Figure 7c). However, the GNs are unevenly distributed, and in either the AFM images of the HPMs or these of the RHPMs, polymer chains with a low contrast are observed (Figure 7a,b), which should be related to the relatively short P4VP block. Because when P4VP chains are short, at the MR of 0.3, some polymer chains complexed with a small quantity of $HAuCl_4$ molecules may either molecularly disperse or form loosely aggregated complexes. It seems that the relatively long P4VP block chains are necessary for the core−shell reversion to form regular RHPMs.

Antonietti et al.[22] reported the preparation of powders (or precipitates) of PS-*b*-P4VP/GNs micelles by addition of methanol into the solution of PS-*b*-P4VP/GNs micelles in toluene. However, in the present study, the addition of methanol into PS-*b*-protonated P4VP/GNs micelles in chloroform leads to the core−shell reversion instead of precipitation. We think that such a difference may mainly arise from the difference in the nature of the cores and the shells in different media: PS shell and protonated P4VP/GNs core in chloroform vs PS shell P4VP/GNs core in toluene. The difference in the nature of the core is particularly notable. It is reported that the cores of polymeric micelles are quite different for different polymeric micelles.[34] On the basis of our previous studies, we found that in some cases the core of polymeric micelles formed in a common solvent of a block copolymer stabilized by noncovalent interaction is loosely aggregated.[35] Experimentally, the density of core of polymeric micelles can be approximately evaluated by the value of $\langle D_g \rangle / \langle D_h \rangle$. The values of $\langle D_g \rangle / \langle D_h \rangle$ for PS-*b*-P4VP/$HAuCl_4$ micelles was measured by static and dynamic light scattering to be 0.91, indicating that the density of the core is relatively low.[34] However, the $\langle D_g \rangle / \langle D_h \rangle$ value for the HPMs is 0.667, which is close to that of block copolymer micelles formed in a selective solvent. Considering that the density of gold (19.6 g/cm^3) is much higher than that of the core of a normal polymeric micelle, encapsulation of a 15 nm GN in the center of the core should decrease the $\langle D_g \rangle / \langle D_h \rangle$ value remarkably.[34] On the other hand, the contribution by the polymeric components (i.e., the HPMs except for GNs) to the $\langle D_g \rangle / \langle D_h \rangle$ should be considerably higher than 0.667. In other words, the protonated P4VP chains surrounding the GNs should be relatively loosely aggregated. It is possible that the loosely aggregated protonated P4VP chains in the HPMs accelerate the diffusion of methanol into the core to dissociate the aggregated protonated P4VP. In a control experiment, we add methanol to the PS-*b*-P4VP/HCl micelles in chloroform, and reversed micelles can be obtained as well.

Conclusions

In conclusion, the micellization of PS-*b*-P4VP in chloroform can be induced by the complexation between the P4VP blocks and $HAuCl_4$, forming polymeric micelles with PS being the shell and P4VP/$HAuCl_4$ complex being the core. Reduction of $HAuCl_4$ molecules within the core using hydrazine hydrate leads to the formation of HPMs containing a 15 nm GN in the core. The resultant HPMs are quite stable in chloroform when the P4VP chains are fully protonated by addition of hydrochloric acid. Continuous addition of methanol into the solution of the HPMs until the VR of methanol to chloroform being 9/1 leads to the core−shell reversion, forming vesicle-like RHPMs with PS being the wall and protonated P4VP/GNs being the shell. We also demonstrate in this study that the GNs can be either stabilized within the shell for months by protonation or released from the shell by deprotonation of the P4VP blocks. The present approach to prepare HPMs with GNs attached to the shell has an advantage over other methods, i.e., an easy control of the size and size distribution of GNs by using the micelle cores as nanoreactors. Besides, the phenomenon that there is no an intermediate state of molecularly dispersed block copolymer in the solution between the HPMs and the RHPMs during the core−shell reversion is novel (further study is needed). We believe that the results of the present study may have potential applications in related theoretical and practical problems such as catalysis and sensors based on GNs.

Acknowledgment. The authors are grateful to the financial support from the National Science Foundation of China (20574014, 20528405).

Supporting Information Available: Experimental details. This material is available free of charge via the Internet at http://pubs.acs.org.

References and Notes

(1) Henselwood, F.; Wang, G. C.; Liu, G. J. *J. Appl. Polym. Sci.* **1998**, *70*, 397−408.
(2) Allen, C.; Han, J. N.; Yu, Y. S.; Maysinger, D.; Eisenberg, A. *J. Controlled Release* **2000**, *63*, 275−286.
(3) Jones, M. C.; Leroux, J. C. *Eur. J. Pharm. Biopharm.* **1999**, *48*, 101−111.
(4) Antonietti, M.; Goltner, C. *Angew. Chem., Int. Ed.* **1997**, *36*, 910−928.
(5) Antonietti, M.; Forster, S.; Hartmann, J.; Oestreich, S. *Macromolecules* **1996**, *29*, 3800−3806.
(6) Liu, S. Y.; Weaver, J. V. M.; Save, M.; Armes, S. P. *Langmuir* **2002**, *18*, 8350−8357.
(7) Sidorov, S. N.; Bronstein, L. M.; Kabachii, Y. A.; Valetsky, P. M.; Soo, P. L.; Maysinger, D.; Eisenberg, A. *Langmuir* **2004**, *20*, 3543−3550.
(8) Selvan, S. T.; Spatz, J. P.; Klok, H. A.; Moller, M. *Adv. Mater.* **1998**, *10*, 132−134.
(9) Antonietti, M.; Forster, S.; Oestreich, S. *Macromol. Symp.* **1997**, *121*, 75−88.
(10) Sakai, T.; Alexandridis, P. *J. Phys. Chem. B* **2005**, *109*, 7766−7777.
(11) Kuo, P. L.; Chen, C. C.; Jao, M. W. *J. Phys. Chem. B* **2005**, *109*, 9445−9450.
(12) Sidorov, S. N.; Bronstein, L. M.; Valetsky, P. M.; Hartmann, J.; Colfen, H.; Schnablegger, H.; Antonietti, M. *J. Colloid Interface Sci.* **1999**, *212*, 197−211.
(13) Bronstein, L. M.; Sidorov, S. N.; Gourkova, A. Y.; Valetsky, P. M.; Hartmann, J.; Breulmann, M.; Colfen, H.; Antonietti, M. *Inorg. Chim. Acta* **1998**, *280*, 348−354.
(14) Porta, F.; Prati, L.; Rossi, M.; Coluccia, S.; Martra, G. *Catal. Today* **2000**, *61*, 165−172.
(15) Mirkin, C. A.; Letsinger, R. L.; Mucic, R. C.; Storhoff, J. J. *Nature (London)* **1996**, *382*, 607−609.
(16) Shenhar, R.; Norsten, T. B.; Rotello, V. M. *Adv. Mater.* **2005**, *17*, 657−669.
(17) Mayer, A. B. R.; Mark, J. E. *Colloid Polym. Sci.* **1997**, *275*, 333−340.
(18) Mayer, A. B. R.; Mark, J. E. *Polym. Prepr. (Am. Chem. Soc., Polym. Chem. Div.)* **1996**, *74*, 459−460.
(19) Mei, Y.; Sharma, G.; Lu, Y.; Ballauff, M.; Drechsler, M.; Irrgang, T.; Kempe, R. *Langmuir* **2005**, *21*, 12229−12234.
(20) Jaramillo, T. F.; Baeck, S. H.; Cuenya, B. R.; McFarland, E. W. *J. Am. Chem. Soc.* **2003**, *125*, 7148−7149.
(21) Lu, Y.; Mei, Y.; Drechsler, M.; Ballauff, M. *Angew. Chem., Int. Ed.* **2006**, *45*, 813−816.
(22) Antonietti, M.; Wenz, E.; Bronstein, L.; Seregina, M. *Adv. Mater.* **1995**, *7*, 1000−1005.
(23) Cheng, W. L.; Wang, E. *J. Phys. Chem. B* **2004**, *108*, 24−26.
(24) Peng, H. S.; Chen, D. Y.; Jiang, M. *Langmuir* **2003**, *19*, 10989−10992.
(25) Peng, H. S.; Chen, D. Y.; Jiang, M. *J. Phys. Chem. B* **2003**, *107*, 12461−12464.
(26) Chu, B.; Wang, Z.; Yu, J. *Macromolecules* **1991**, *24*, 6832−6838.
(27) Chen, D. Y.; Peng, H. S.; Jiang, M. *Macromolecules* **2003**, *36*, 2576−2578.
(28) Yao, X. M.; Chen, D. Y.; Jiang, M. *J. Phys. Chem. B* **2004**, *108*, 5225−5229.
(29) Mossmer, S.; Spatz, J. P.; Moller, M.; Aberle, T.; Schmidt, J.; Burchard, W. *Macromolecules* **2000**, *33*, 4791−4798.
(30) Gao, Z. S.; Desjardins, A.; Eisenberg, A. *Macromolecules* **1992**, *25*, 1300−1303.
(31) Li, X. H.; Li, Y. C.; Tan, Y. W.; Yang, C. H.; Li, Y. F. *J. Phys. Chem. B* **2004**, *108*, 5192−5199.
(32) Mayer, A. B. R. *Mater. Sci. Eng., C* **1998**, *6*, 155−166.
(33) Zhang, G. Z.; Liu, L.; Zhao, Y.; Ning, F. L.; Jiang, M.; Wu, C. *Macromolecules* **2000**, *33*, 6340−6343.
(34) Tu, Y. F.; Wan, X. H.; Zhang, D.; Zhou, Q. F.; Wu, C. *J. Am. Chem. Soc.* **2000**, *122*, 10201−10205.
(35) Jia, X.; Chen, D. Y.; Jiang, M. *Chem. Commun.* **2006**, 1736−1738.

MA062373B